Bounding the top Yukawa with Higgs-associated single-top production

Christoph Englert[1,*] and Emanuele Re[2,†]

[1]SUPA, School of Physics and Astronomy, University of Glasgow, Glasgow, G12 8QQ, United Kingdom

[2]Rudolf Peierls Centre for Theoretical Physics, Department of Physics, University of Oxford, Oxford, OX1 3NP, United Kingdom

After the discovery of the 125 GeV scalar boson with gauge properties similar to the Standard Model Higgs, the search for beyond the SM interactions will focus on studying the discovered particles' coupling properties more precisely and shedding light on the relation of fermion masses with the electroweak vacuum. The large mass of the top quark and the SM-predicted order one top Yukawa coupling is a natural candidate for BSM physics, though experimentally challenging to constrain. In this paper, we argue that investigating angular correlations in $pp \to tHj$ production provides an excellent handle to constrain the top Yukawa coupling y_t via direct measurements, even when we focus on rare exclusive final states. We perform a hadron-level analysis and show that we may expect to constrain $y_t \gtrsim 0.5\, y_t^{\rm SM}$ at 95%-99% confidence level at the high luminosity LHC using semi-leptonic top decays and $H \to \gamma\gamma$ alone, by employing a two-channel measurement approach.

arXiv:1402.0445v2 [hep-ph] 9 May 2014

I. INTRODUCTION

The discovery of a 125 GeV scalar boson [1, 2] marks a milestone in our understanding of the mechanism of electroweak (EW) symmetry-breaking. In order to unambiguously decipher the role exactly played by the corresponding scalar field in breaking the EW symmetry, it is mandatory to measure as accurately as possible the couplings between the Higgs boson and all other SM particles we already know, as well as the Higgs self-coupling. This programme has already started and, as new data becomes available, results are continuously updated by the ATLAS and the CMS collaborations [3, 4], as well as by the theoretical community [5].

If no striking direct evidence for new physics will be found within the first few years of the next LHC phase, an accurate extraction of the Higgs couplings will become even more important than it is already now: looking for deviations from the SM values will then be our main route to probe (indirect) manifestations of new physics. In other words, if no other new particle beside the Higgs is found, one of the main goals in the near future will be precision physics in the Higgs sector, using data from the LHC as well as from other experiments (see *e.g.* [6–8] for discussions).

The extraction of the Higgs mass, quantum numbers and couplings (and the related confidence levels) from LHC data is usually performed by minimizing a chi-squared distribution associated with a global fit to the data. Although theoretically debatable, it is common practice to choose the coefficients representing deviations from the SM values of the Higgs couplings as free parameters in this procedure [3–5]. The results of such fits can be used to directly constrain the parameter space of specific extensions of the SM, or to map deviations from the SM onto the coefficients of higher-dimensional operators, using an effective field theory language.

The ultimate accuracy of this approach will be limited by systematics, statistics, and theoretical uncertainties in the prediction of signal and background cross sections and branching ratios (these are the quantities used to define the so-called signal strengths, *i.e.* the quantities used to obtain the set of Higgs couplings for which the best fit to data is obtained).

A precise (in)direct measurement of the top Yukawa coupling y_t (or at least direct sensitivity to it) is of fundamental importance. The large mass hierarchy between the different quark generations is not explained in the SM and the top mass being close to the electroweak scale can be interpreted as a hint for TeV-scale physics beyond the SM. Well-known examples of modified Higgs-top interactions are the two Higgs doublet model, the MSSM and composite Higgs scenarios where the size of the top mass is explained by linear mixing effects with new TeV-scale top partners [9–11]. In the latter models, the contribution from the Higgs vacuum expectation value is less constrained, and the top Yukawa can be smaller than the SM value, $y_t < y_t^{\rm SM}$.

In the light of the currently available data, the aforementioned fits are sensitive to y_t mainly via the measurement of the cross section for Higgs production in gluon fusion as well as the Higgs to diphoton branching ratio. Both the $gg \to H$ and $H \to \gamma\gamma$ processes are loop-mediated, and therefore the extraction of y_t from these measurements is potentially very sensitive to effects of to yet-to-be discovered states; large deviations from the SM expectations in these channels would be a strong hint of new physics. However, if the Higgs is indeed a pseudo-Nambu Goldstone boson, the effective ggH and $\gamma\gamma H$ couplings can still be SM-like, because higher dimension operators are suppressed by the approximate shift symmetry of the Goldstone Higgs doublet. In such a case, a direct measurement of the top

*Electronic address: christoph.englert@glasgow.ac.uk
†Electronic address: emanuele.re@physics.ox.ac.uk

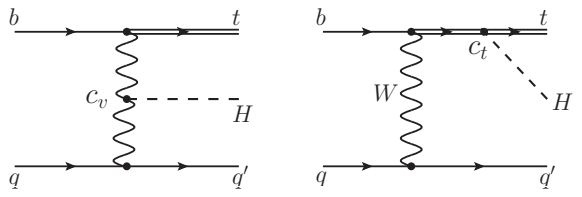

FIG. 1: Feynman diagrams for tree-level production of single-top + Higgs. The diagram on the left (right) is proportional to C_{WWH} (C_{ttH}).

Yukawa coupling provides valuable information necessary to break the measurements' degeneracy in the extended top sector, where an enlarged (global) symmetry is responsible for the "conspiracy" to SM-like ggH and $\gamma\gamma H$ couplings [10]. This is especially true when the top partners fall outside the LHC coverage or are masked by experimental systematics. Similar phenomenological implications also hold for exotic models with Higgs triplets, see *e.g.* [12].

The above examples clearly show that, despite being extremely interesting and seminal to Higgs physics, the presence of potentially unknown loop effects (in addition to the LHC being unable to directly measure the total Higgs width to satisfactory accuracy) makes the ggH and $\gamma\gamma H$ not ideal to set theoretically solid bounds on the tree-level $t\bar{t}H$ coupling in a model-independent way. It is therefore important to complement these indirect measurements with direct observations of processes where y_t enters already at tree-level.

At the LHC there are two basic processes which serve this purpose: $t\bar{t}$ associated production ($pp \to t\bar{t}H$) and Higgs + single-top production ($pp \to tHj$). An experimental observation of these production channels is challenging because cross sections are in general quite small ($t\bar{t}H$ has the smallest cross section among the standard Higgs-production processes), and, moreover, backgrounds are generically hard to suppress.

Not surprisingly, until new techniques were introduced few years ago [13–17], there were serious doubts even about being able to observe the $pp \to t\bar{t}H$ signal on top of the dominant backgrounds [18] in the first place. Associated single-top production [19] has an even slightly smaller cross section, and, for similar reasons, has received little attention [20, 21] until recently. Despite of the aforementioned experimental difficulties, given the importance of the top Yukawa as a parameter potentially probing new physics, it is worthwhile to investigate the signatures that might allow its direct extraction. Although current projections indicate that a direct measurement will be challenging (at least with traditional analysis techniques), studying the extent to which y_t can be directly bounded remains a relevant and timely question.

The purpose of this paper is to perform a phenomenological analysis of a signal based on associated single-top production, and to discuss in how far we can use a successful signal and background analysis to constrain y_t. We will show that despite the fact that the top semileptonic and the $H \to \gamma\gamma$ branchings are not the dominant ones, it is still possible to obtain limits for the high-luminosity LHC.

In Sec. II we briefly overview the phenomenology of Higgs + single-top production. In Sec. III we detail our analysis and present our results, before we summarize our findings and conclude in Sec. IV.

II. HIGGS + SINGLE-TOP PHENOMENOLOGY

At the lowest order in perturbation theory, the hadroproduction of Higgs + single-top arises from the Feynman diagrams shown in Fig. 1.* These two diagrams show that the top Yukawa enters at tree-level, and, moreover, because of the interference taking place at the amplitude level, the squared matrix-element contains a term linear in $C_{ttH}C_{WWH}$, where we have parameterized the deviations from the SM Higgs couplings

$$C_{ttH}^{\rm SM} = -\frac{y_t}{\sqrt{2}} = -\frac{m_t}{v_{\rm SM}}\,, \qquad C_{WWH}^{\rm SM} = g_W^2\frac{v_{\rm SM}}{2} \tag{1}$$

as

$$C_{ttH} = c_t \times C_{ttH}^{\rm SM}\,, \qquad C_{WWH} = c_v \times C_{WWH}^{\rm SM}\,. \tag{2}$$

Since the Higgs insertion at a fermion line introduces a chirality flip, dialling C_{ttH} away from its SM value is tantamount to populating different (anti-)top helicity states that in turn result in different top decay patterns in comparison to the SM. It is the combination of these effects that motivates the tHj channel as a unique tool for establishing a direct measurement of sign and size of the top Yukawa as opposed to $pp \to t\bar{t}H$. Hence it is no surprise that tHj production has recently received considerable attention from the theory community [25–28].

Recent global fits of the Higgs couplings are now ruling out the $c_t < 0$ possibility well above the 95% CL [29, 30], and start constraining the $c_t > 0$ parameter region with available Higgs data.† Very recently it has also been noticed that a $\mathcal{CP}$-violating component to the top Yukawa coupling ($\sim i\,\tilde{C}_{ttH}(\bar{t}\gamma_5 t)\,H$) can be studied in this channel [7], complementing bounds obtained from low-energy experiments [6]. We do not include this possibility in

* In this paper we work in the 5-flavour scheme, which means that in the initial state we consider massless b-quark. For this reason, we neglect diagrams with the Higgs being emitted off b-quarks. In the single-top literature, it is known that a 5-flavour approach compares well with a computation in the 4-flavour scheme, that would allow in turn a better description of the spectator b-jet [22–24].

† Obviously direct measurement constraints are statistically limited in the present case and will be not as tight as the indirectly obtained ones.

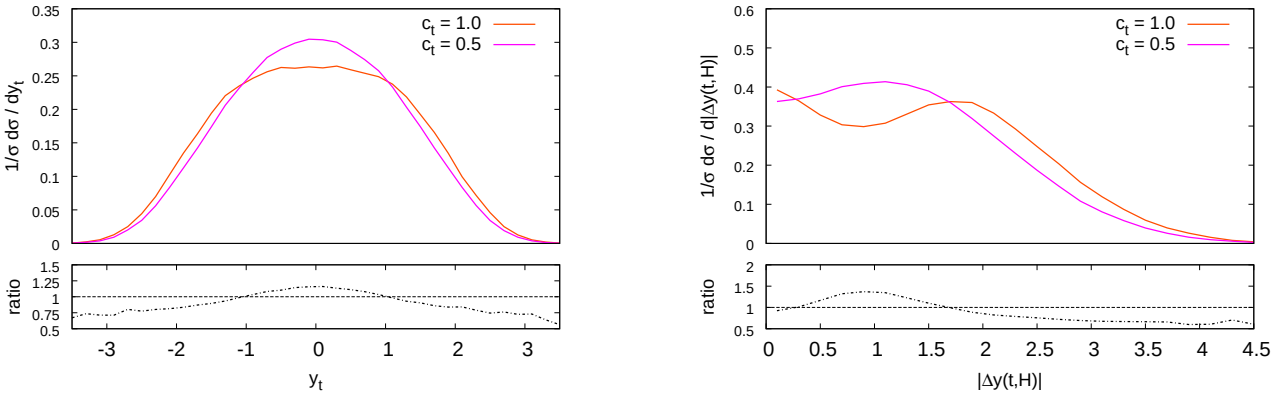

FIG. 2: Parton level leading-order distribution of the reconstructed top quark rapidity y_t (left) and the rapidity distance between the top quark and the Higgs boson $|\Delta y(t,H)|$ (right). Plots have been obtained using the cuts in Eq. 3 and have been normalized to unity. In the lower insets the ratio between the $c_t = 0.5$ and the SM distributions is shown.

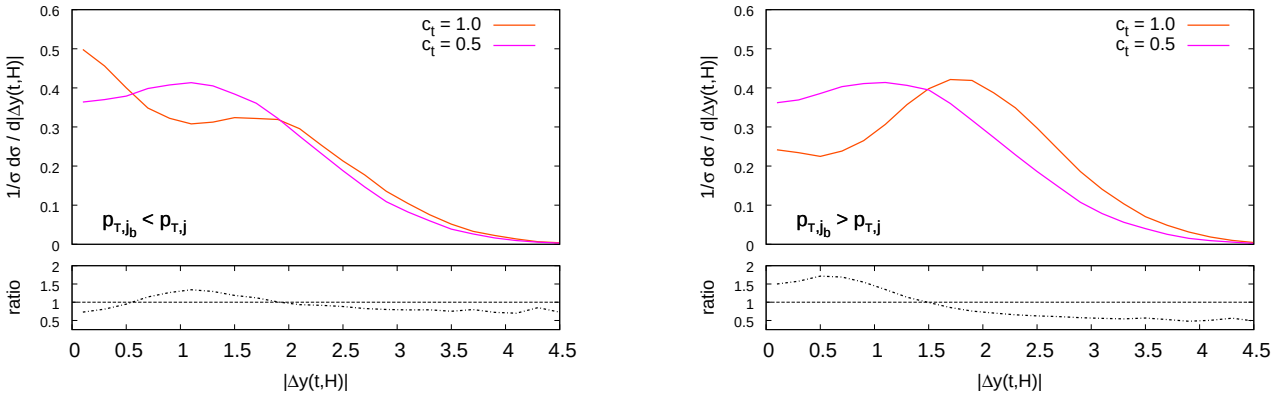

FIG. 3: Rapidity distance between the top quark and the Higgs boson in presence of the cuts in Eq. 3. On the left (right) panel, the requirement of having a b-jet softer (harder) than the light jet is enforced.

this paper, but we expect that similar implications can be formulated in the $\mathcal{CP}$-violating context, too.

If also C_{WWH} is assumed to be a free parameter, then deviations from the SM expected cross section could be used to set bounds in the (c_v, c_t) plane. Here however, we work in the assumption of having a precise measure of c_v: this is a reasonable and realistic assumption, since there are several other processes which will allow to probe C_{WWH} independent from the process we are interested in [31], and definitely with a shorter time scale with respect to that needed to accumulate the luminosity required to observe tHj.

As mentioned above, we are interested in the possibility to observe and measure the tHj cross section by looking at the $H \to \gamma\gamma$ decay. Because this branching ratio depends on C_{WWH} and C_{ttH}, the measurement of the total cross section with a diphotonic final state cannot be straightforwardly translated into a limit on the top Yukawa coupling. We consider two ways to deal with this issue. The first possibility is to just rely on the fact that by the time when this measurement will be possible, the LHC will have completed a "legacy" measurement of the $H \to \gamma\gamma$ branching, which can be used as an input for our proposed analysis. Alternatively, one can also include the dependence on the c_t factor entering in $H \to \gamma\gamma$, assuming that only the top Yukawa is allowed to float (in which case the total Higgs width stays approximately unchanged once C_{WWH} is fixed, because the dominant $H \to b\bar{b}, c\bar{c}, \tau\bar{\tau}$ and VV partial widths are fixed). We will report two different confidence limits for the Yukawa coupling: The first limit follows form a SM-like $H \to \gamma\gamma$ branching ratio and the second one includes the back-reaction of the modified top Yukawa coupling on the Higgs decay phenomenology.

We will derive these constraints from characteristic angular observables of the exclusive tHj final state after showering, hadronization and signal vs. background enhancing selection cuts. In our study we have identified several variables sensitive to the size of c_t. For this paper, we have chosen $R(H, j_b) = \sqrt{\Delta\phi(H, j_b)^2 + \Delta y(H, j_b)^2}$,

i.e. the distance between the b jet and the reconstructed Higgs boson in the (y, ϕ) plane as a single discriminating variable, since this observable optimizes the discriminative power between different signal hypothesis in the presence of realistic cuts, as we will show in the next section. We will also discuss the sensitivity of $\Delta y(H, j_b)$ to the value of c_t.

To understand the typical kinematics of the final state, we start by reminding the reader that the cross section for tHj production is minimal for a SM-like top Yukawa value ($c_t = 1$). This is due to destructive interference between the diagrams of Fig. 1 becoming maximal [25]. It is instructive to study some leading-order parton-level distributions [32] in presence of very generic cuts:

$$\begin{aligned} \text{lepton} &: \; p_{T,\ell} \geq 10\text{GeV}, \; |\eta_\ell| < 2.5\,, \\ \text{photons} &: \; p_{T,\gamma} \geq 30\text{GeV}, \; |\eta_\gamma| < 2.5\,, \; R(\gamma,\gamma) > 0.1\,, \\ \text{jets} &: \; p_{T,j} > 20\text{GeV}, \; |\eta_j| < 4.5\,. \end{aligned} \tag{3}$$

Jets are obtained clustering the final state partons with FastJet [33], using the anti-k_T algorithm [34] with $R = 0.4$.

First of all we notice that the light jet associated to the light quark current is typically produced at relatively small transverse momentum ($p_{T,j}$ peaks at ~ 40 GeV) and high rapidity ($|y_j| \sim 3$). Hence cutting away events with central light jets will not deplete significantly the signal, helping therefore in enhancing the signal vs. background ratio. We also notice that typically the top quark and the light jet lie in opposite hemispheres, and as a consequence the heavy objects in the final state are distributed such that the top quark is typically further away in rapidity from the light jet than the Higgs boson. In the next section, we will make use of these properties of the signal's kinematics to design a cut flow that affects the signal rates as less as possible.

In the left panel of Fig. 2 the leading-order distribution of the reconstructed top (and anti-top) rapidity is shown[‡] for the two representative values of c_t that will be used in the following, after applying the cuts in Eq. 3. Since we want to concentrate on shape differences, here we show unit-normalized curves, but we stress that the total cross-section for $c_t = 0.5$ is a factor ~ 1.5 larger than the SM value. Together with this observation, the plot in the left panel of Fig. 2 shows that the interference term is significantly bigger in size, and negative, when tops are central: consequently it is clear that the smaller c_t is, the more central the top quarks are, and, conversely, tops are fairly uniformly distributed in the central rapidity region when $c_t = 1$. These observations apply as well for the reconstructed Higgs (not shown): in the SM scenario, y_H is essentially flat for $y_H \in [-1, 1]$, whereas for "BSM" scenarios the Higgs rapidity tends to peak at 0.

In the right panel of Fig. 2 we show how this pattern translates to the rapidity distance between the top and the Higgs, which is related to the observables in which eventually we will be interested, *i.e.* distances between the reconstructed Higgs and the hardest b-jet. In the SM case the negative interference affects very sizeably the $|\Delta y(t, H)| \sim 1$ region, creating a visible shape difference between the two signal hypothesis. As we will observe in Sec. III, the slope shown in the ratio panel on the right persists even in presence of the other cuts that will be introduced to enhance S/B, and affects also $R(H, j_b)$ and $\Delta y(H, j_b)$ too, which we will use to set exclusion limits.

In anticipation of the main results, we also show how the $\Delta y(t, H)$ distributions look when we split the total cross section by requiring the b-jet to be harder (softer) than the light jet. Fig. 3 shows that, when $p_{T,j_b} < p_{T,j}$, the above picture is not qualitative changed. However, for $p_{T,j_b} > p_{T,j}$, the Higgs boson and the top quark are much closer in rapidity when $c_t = 0.5$, as shown in the right panel of Fig. 3. This is due to the fact that to have hard b-jets, the parent tops need to be more central: when $c_t = 1$, this situation is strongly disfavored by the negative interference, as commented above, whereas a large part of the cross section in the $c_t = 0.5$ case is concentrated in this phase-space region, as shown in the main panels. In the next section we will use this very large shape differences in Δy distributions, in the regime where $p_{T,j_b} > p_{T,j}$, as an extra-handle to set stronger constraints on the top Yukawa.

III. PROSPECTIVE SENSITIVITY AND DISCOVERY THRESHOLDS AT 14 TEV

In the following we perform a hadron-level analysis of the process $pp \to (t \to \ell b\nu)(H \to \gamma\gamma)j$, $\ell = e, \mu$, at 14 TeV with a target luminosity of 3/ab. This will allow us give an estimate of the discriminative power that is encoded in angular observables after realistic selection criteria have been applied.

We investigate an exclusive final state that is obviously the cleanest channel to observe tHj production yet statistically limited due to the small $H \to \gamma\gamma$ branching ratio. Side-band analysis techniques are applicable and we can expect that systematic uncertainties in this final state are small compared to multi b-tagged events that have been discussed in the literature in the context of parton-level analyses [20, 25, 26, 28]. We include the following dominant irreducible and fake (jet faking b-jets, jets faking photons[§]) backgrounds: $W^\pm(H \to \gamma\gamma)$+jets, $W^\pm\gamma\gamma$+jets, $t\gamma\gamma$+jets, $\bar{t}\gamma\gamma$+jets, $t\bar{t}\gamma\gamma$+jets, $t\bar{t}(H \to \gamma\gamma)$+jets, $t\gamma$+jets, and $\bar{t}\gamma$+jets.

All event samples are generated with MadGraph [36],

[‡] Unless otherwise stated, all the following distributions are obtained by summing the cross sections for tHj and $\bar{t}Hj$ production.

[§] We use a flat factor of 1/1000 for the jets faking photons [35].

using the default CTEQ6L1[37] parton densities, and are subsequently showered with HERWIG++ [38]. Quite obviously, a lot of systematic limitations that are discussed in the context of $t\bar{t}H$ analyses also impact this analysis, most notably the issues of heavy flavor contributions that are still under investigation presently [39]. The final state we consider in this section will clearly minimize the sensitivity to these effects compared to multi b-tagged final state, but heavy flavor production and tagging still deserves a more detailed investigation in the context of tHj production once the theoretical and experimental questions raised in [39] are settled. A realistic in-depth analysis of the corresponding uncertainties is currently not available and beyond the scope of this section, therefore our results need to be understood with a pinch of salt.

Our selection criteria closely follow the event topology that results from the Feynman diagrams in Fig. 1: we typically deal with a central b jet and a forward jet that are balanced by the Higgs. Since we only have electromagnetic calorimetry in the central part of the detector ($|\eta| < 2.5$), we lose a fraction of the signal due to the reconstruction in the central part of the detector. This is unavoidable also for other decay modes, *e.g.* for $H \to b\bar{b}$, because b-jet identification relies on vertexing in the central part of the detector too. We will continue to focus on $c_t = 0.5$ for illustration and also comment on $y_t > y_t^{\rm SM}$ at a later stage. The latter case is typically more complicate to constrain when the back-reaction on $H \to \gamma\gamma$ is included.

In the actual analysis, we define isolated leptons and photons for tracks which have less than 10% energy deposit relative to the tracks' transverse momentum in a cone of size $\Delta R = 0.1$. Leptons, photons and jets are then selected using the same basic cuts reported in Eq. 3. We ask here for *exactly* one lepton, two photons, and two jets (this reduces the reducible backgrounds but also the signal).

The two photons need to be isolated $R(\gamma_1, \gamma_2) > 0.1$ and need to reproduce the Higgs mass of 125 GeV within $|m(\gamma_1, \gamma_2) - 125 \text{ GeV}| < 10$ GeV. The jets need to be separated by $R(j_1, j_2) \geq 2$. Subsequently, we use a two channel approach to formulate limits on the top Yukawa coupling, described in the following:

1.) We order the jets in hardness $p_{T,j_1} > p_{T,j_2}$. j_2 needs to be central with $|\eta_{j_2}| < 2.5$, and needs to pass a b-tag, whereas j_1 is in the forward region $|\eta_{j_1}| > 1.0$. We use a working point with an efficiency of 85% and a fake rate of 10% [40]. The isolated lepton and jet j_2 needs to have an invariant mass $m(j_2, \ell) < 200$ GeV and j_1 needs to be separated from the lepton by $R(\ell, j_1) \geq 1$, and from the reconstructed Higgs ($p_H = p_{\gamma_1} + p_{\gamma_2}$) by $R(H, j_1) \geq 2.5$.

This cut flow is designed in such a way that we gain sensitivity to $c_t = 1$ over the background.¶ Specifically, in this "SM region" we expect $\mathcal{O}(10)$ signal events (see Tab. I), that can in principle be used to calibrate the measurement. We refer to this selection as "Channel 1" (CH1). The second selection is better tailored to BSM-induced effects, yet statistically independent from CH1:

2.) We order the jets $p_{T,j_2} > p_{T,j_1}$ and proceed subsequently exactly as described in 1.). In particular, this amounts to events with harder b jets, and invariant j_2, ℓ mass cuts on the harder jet.

We refer to this selection as "Channel 2" (CH2).

After these steps we end up with cross sections of the two searches as detailed in Tab. I.

As explained previously, an appropriate choice of a discriminative collider observable that encodes sensitivity to the top Yukawa coupling is the rapidity difference between the reconstructed Higgs and the b-jet. It also feeds into the lego-plot separation $R(H, j_b)$ which, following our earlier discussion, is also sensitive to the top quark Yukawa coupling, as can be seen in Figs. 4 and 5.

Note that our cut flow does not directly cut on this observable, although the requirements $p_{T,j_b} \lesseqgtr p_{T,j}$ changes the behaviour of $R(H, j_b)$ and $\Delta y(H, j_b)$, as anticipated in Sec. II. As can be seen in Fig. 5, in the CH2 scenario, a better discrimination of c_t can be achieved.

To compute a confidence level interval for the top Yukawa coupling we perform a binned log-likelihood analysis [41, 42] as invoked by the experiments (see *e.g.* [3, 4, 43] for details and validation) on the basis of the distributions of Fig. 4. We use the CLs method [44] to formulate a lower limit on the top Yukawa interactions. Since the top Yukawa coupling interferes destructively with the remaining contributions in Fig. 1, we obtain a larger cross section for $y_t < y_t^{\rm SM}$ for fixed top and Higgs masses and widths and can formulate constraints.

Scanning over different signal event samples with varied y_t, keeping track of the differential cross section modifications, we compute a lower limit (keeping $C_{WWH} = 1$)

$$c_t \gtrsim 0.5 \text{ at } 67\% \text{ CLs } [80\% \text{ CLs}]\,, \tag{4}$$

Channel 1	$\sigma_B = 10.09$ ab	$\sigma_S = 2.92$ ab	$c_t = 1.0$
		$\sigma_S = 4.80$ ab	$c_t = 0.5$
Channel 2	$\sigma_B = 6.3$ ab	$\sigma_S = 2.02$ ab	$c_t = 1.0$
		$\sigma_S = 4.42$ ab	$c_t = 0.5$

TABLE I: Signal and background cross sections as for the two selections as described in the text.

¶ In particular the cuts on the lego-plot separations among the various objects help in reducing the backgrounds without depleting the signal too much: as we noticed in Sec. II, the signal cross section is indeed characterized by "large" distances between the light jet and the other heavy objects.

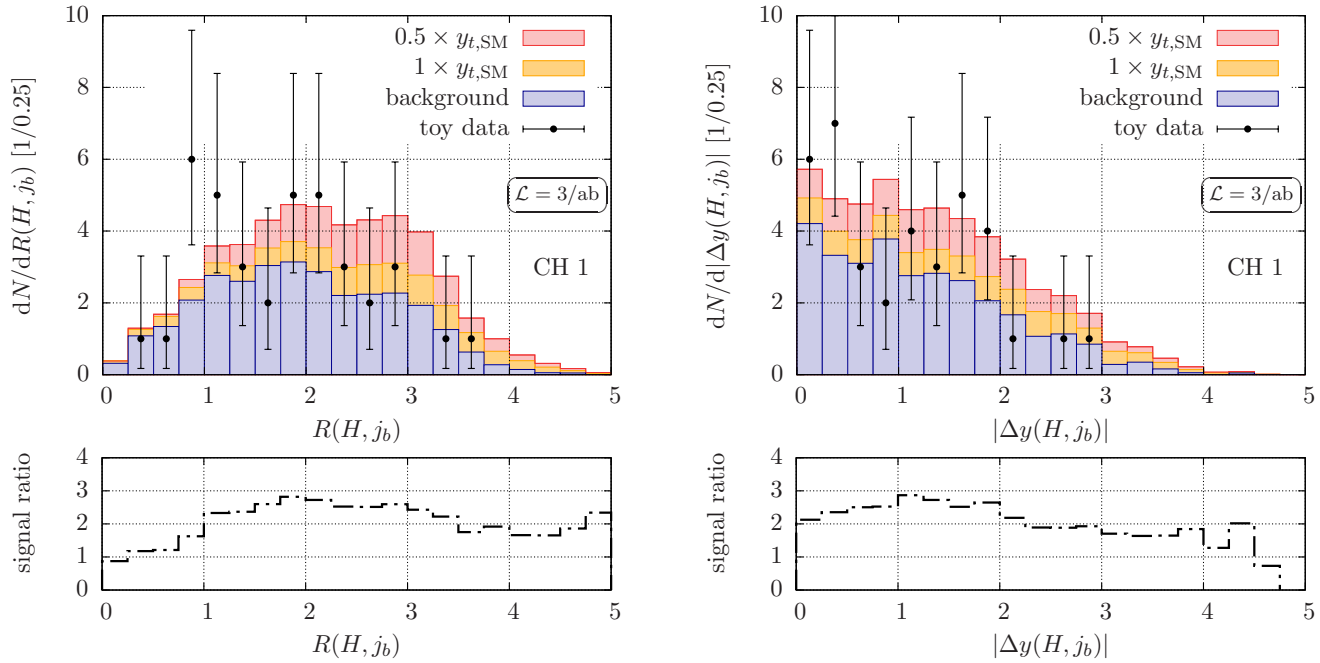

FIG. 4: Lego-plot separation and rapidity difference of the reconstructed Higgs boson and b-tagged jet. We show the expected distribution for a target luminosity of 3/ab after the selection criteria detailed in the text have been applied. To get an idea of the involved statistical uncertainty of such a measurement with an SM-consistent outcome, we include toy data and the 95% Bayesian confidence level error bars around the central values. We use these distributions and MC-sampled toy measurements to compute a confidence level interval for the top quark Yukawa coupling (see text); the $c_t = 0.5$ sample includes a modified $h \to \gamma\gamma$ branching ratio. Note that the signal hypotheses overlap. The background does not contain the modifications due to $c_t < 1$ for illustration purposes.

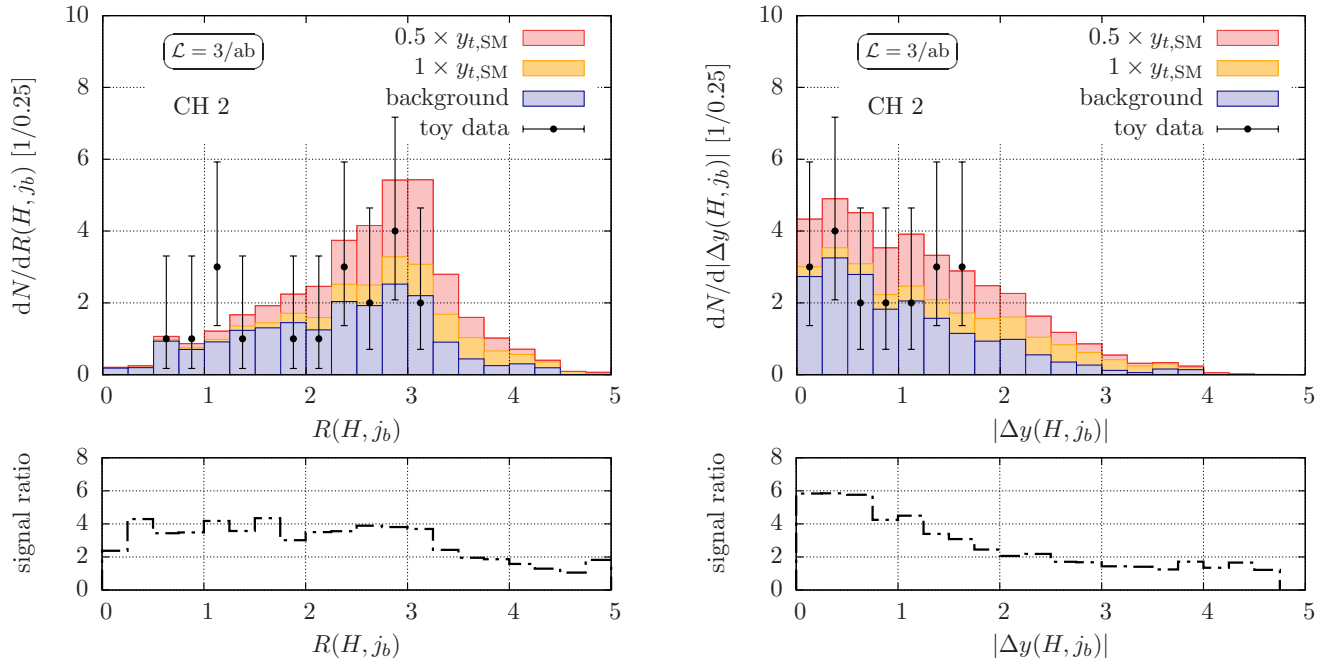

FIG. 5: Same as Fig. 4 for a measurement performed in channel 2 as defined in the text.

where the number in brackets refers to the confidence level when the modified y_t feeds into $h \to \gamma\gamma$ in the signal sample (for comparison reasons we take Fig. 5 at face value). The differential cross section indeed contains valuable information which is not accessible by only counting events: the confidence level for a CLs test based

on total event counts we only exclude $c_t \lesssim 0.5$ at 58% CLs [73% CLs].

We now include the information of channel 2 to the picture. In this case, as we have explained above in detail, the ratio between ΔR distributions has a different (inverted) shape at small values and provides increased statistical pull. Despite that in this case S/B is not as optimal for the SM scenario as before, we add statistical information that efficiently constrains c_t across the two regions. We end up with confidence levels for our benchmark point (modifications of the Higgs-included background contributions are taken into account)

$$c_t \gtrsim 0.5 \text{ at } 95\% \text{ CLs } [99\% \text{ CLs}]\,. \tag{5}$$

Similarly we can try to formulate an upper bound for y_t. The tHj production cross section starts to grow for $y_t > y_t^{\rm SM}$, but the $H \to \gamma\gamma$ branching ratio falls quickly and stays small because of a increasingly preferred gluonphillic Higgs decay. This leads to a much looser constraint when we include the back-reaction of the modified top Yukawa coupling on the diphoton branching. We obtain

$$c_t \lesssim 1.6 \text{ at } 95\% \text{ CLs } [85\% \text{ CLs}]\,, \tag{6}$$

where the number in brackets corresponds again to the constraint with modified $H \to \gamma\gamma$.

IV. SUMMARY

The late discovery of the Higgs boson provides us a unique opportunity to put the SM hypothesis to the ultimate test: Is the Higgs boson really the one predicted by the SM or is it the harbinger of physics beyond the SM? Theoretical prejudice based on TeV scale naturalness inevitably forces the latter interpretation upon us. Given that the top quark is of crucial importance for natural TeV scale due to its large Yukawa interaction y_t, the top-Higgs sector is a well-motivated playground to look for deviations from the SM expectation.

In this paper, we have argued that we should be able to constrain the Yukawa coupling at the high luminosity LHC (3/ab) at 14 TeV, even if we focus on rare final states of tHj production. Tree-level destructive interference effects steered by y_t result in modified angular correlations and signal cross sections motivate measurements based on angular correlation-inspired collider observables as well-adapted search strategies for deviations from the SM. To maximize the sensitivity to $y_t \neq y_t^{\rm SM}$, we employ an analysis approach that is based on two complementary selections of the exclusive rare final states that results from leptonic top decays and $H \to \gamma\gamma$. The first one is a "traditional" signal vs. background discrimination that adapts to the SM expectation and seeks to gain as much signal events as possible in the SM-context (and calibrating the measurement). The second complementary selection adapts to a phase space region that is mostly dominated by $y_t \neq y_t^{\rm SM}$-induced modifications of the showered differential angular observables. Combining the two selections we have shown in detail that $y_t \lesssim 0.5\, y_t^{\rm SM}$ can be excluded at 95%-99% CL and similarly $y_t \gtrsim 1.6\, y_t^{\rm SM}$ at 85%-95% CL, already in this channel (depending on the assumptions made on the $H \to \gamma\gamma$ branching). Since we do not rely on any details of the Higgs system, our approach can straightforwardly be generalized to other Higgs decay modes.

Acknowledgments

CE thanks B. Aacharya, J. Ferrando, M. Takeuchi, and M. Spannowsky for helpful conversations. ER is grateful to U. Haisch for giving an initial motivation to look into Refs. [25, 26], and for several interesting discussions, and to B. Mele for an useful and encouraging discussion in Trento. CE is supported in parts by the IPPP Associateship programme.

[1] The ATLAS collaboration, Phys. Lett. B **716** (2012) 1.
[2] The CMS collaboration, Phys. Lett. B **716** (2012) 30.
[3] The ATLAS collaboration, ATLAS-CONF-2012-170.
[4] The CMS collaboration, CMS-PAS-HIG-12-045.
[5] A. Azatov, R. Contino and J. Galloway, JHEP **1204** (2012) 127. P. P. Giardino, K. Kannike, M. Raidal and A. Strumia, Phys. Lett. B **718** (2012) 469. J. Ellis and T. You, JHEP **1209** (2012) 123. J. R. Espinosa, C. Grojean, M. Muhlleitner and M. Trott, JHEP **1212** (2012) 045. T. Plehn and M. Rauch, Europhys. Lett. **100**, 11002 (2012). T. Corbett, O. J. P. Eboli, J. Gonzalez-Fraile and M. C. Gonzalez-Garcia, Phys. Rev. D **87** (2013) 015022. E. Masso and V. Sanz, Phys. Rev. D **87** (2013) 3, 033001. A. Djouadi and G. Moreau, arXiv:1303.6591 [hep-ph].
[6] J. Brod, U. Haisch and J. Zupan, JHEP **1311** (2013) 180 [arXiv:1310.1385 [hep-ph], arXiv:1310.1385].
[7] J. Ellis, D. S. Hwang, K. Sakurai and M. Takeuchi, arXiv:1312.5736 [hep-ph].
[8] R. Contino, M. Ghezzi, C. Grojean, M. Muhlleitner and M. Spira, JHEP **1307** (2013) 035 [arXiv:1303.3876 [hep-ph]].
[9] K. Agashe, R. Contino and A. Pomarol, Nucl. Phys. B **719** (2005) 165 [hep-ph/0412089].
[10] A. Azatov, R. Contino, A. Di Iura and J. Galloway, Phys. Rev. D **88** (2013) 075019 [arXiv:1308.2676 [hep-ph]]. A. Azatov and J. Galloway, Int. J. Mod. Phys. A **28** (2013) 1330004 [arXiv:1212.1380].
[11] S. Dawson and E. Furlan, Phys. Rev. D **86**, 015021 (2012) [arXiv:1205.4733 [hep-ph]].
[12] D. Carmi, A. Falkowski, E. Kuflik and T. Volansky, JHEP **1207** (2012) 136 [arXiv:1202.3144 [hep-ph]]. C. Englert, E. Re and M. Spannowsky, Phys. Rev. D **87**

(2013) 095014 [arXiv:1302.6505 [hep-ph]].
[13] J. M. Butterworth, A. R. Davison, M. Rubin and G. P. Salam, Phys. Rev. Lett. **100** (2008) 242001 [arXiv:0802.2470 [hep-ph]].
[14] T. Plehn, G. P. Salam and M. Spannowsky, Phys. Rev. Lett. **104** (2010) 111801 [arXiv:0910.5472 [hep-ph]].
[15] D. E. Soper and M. Spannowsky, Phys. Rev. D **87** (2013) 5, 054012 [arXiv:1211.3140 [hep-ph]].
[16] D. Curtin, J. Galloway and J. G. Wacker, Phys. Rev. D **88** (2013) 093006 [arXiv:1306.5695 [hep-ph]].
[17] P. Artoisenet, P. de Aquino, F. Maltoni and O. Mattelaer, Phys. Rev. Lett. **111** (2013) 091802 [arXiv:1304.6414 [hep-ph]].
[18] J. Cammin, M. Schumacher, ATL-PHYS-2003-024.
[19] W. J. Stirling and D. J. Summers, Phys. Lett. B **283**, 411 (1992). A. Ballestrero and E. Maina, Phys. Lett. B **299**, 312 (1993). G. Bordes and B. van Eijk, Phys. Lett. B **299**, 315 (1993).
[20] F. Maltoni, K. Paul, T. Stelzer and S. Willenbrock, Phys. Rev. D **64** (2001) 094023 [hep-ph/0106293].
[21] T. M. P. Tait and C. -P. Yuan, Phys. Rev. D **63**, 014018 (2000) [hep-ph/0007298].
[22] J. M. Campbell, R. Frederix, F. Maltoni and F. Tramontano, Phys. Rev. Lett. **102**, 182003 (2009) [arXiv:0903.0005 [hep-ph]].
[23] F. Maltoni, G. Ridolfi and M. Ubiali, JHEP **1207**, 022 (2012) [Erratum-ibid. **1304**, 095 (2013)] [arXiv:1203.6393 [hep-ph]].
[24] R. Frederix, E. Re and P. Torrielli, JHEP **1209**, 130 (2012) [arXiv:1207.5391 [hep-ph]].
[25] S. Biswas, E. Gabrielli and B. Mele, JHEP **1301** (2013) 088 [arXiv:1211.0499 [hep-ph]].
[26] M. Farina, C. Grojean, F. Maltoni, E. Salvioni and A. Thamm, JHEP **1305** (2013) 022 [arXiv:1211.3736 [hep-ph]].
[27] P. Agrawal, S. Mitra and A. Shivaji, JHEP **1312** (2013) 077 [arXiv:1211.4362 [hep-ph]].
[28] S. Biswas, E. Gabrielli, F. Margaroli and B. Mele, JHEP **07** (2013) 073 [arXiv:1304.1822 [hep-ph]].
[29] G. Aad *et al.* [ATLAS Collaboration], Phys. Lett. B **726** (2013) 88 [arXiv:1307.1427 [hep-ex]].
[30] S. Chatrchyan *et al.* [CMS Collaboration], arXiv:1312.1129 [hep-ex].
[31] M. Klute, R. Lafaye, T. Plehn, M. Rauch and D. Zerwas, Europhys. Lett. **101** (2013) 51001 [arXiv:1301.1322 [hep-ph]].
[32] J. Campbell, R. K. Ellis and R. Rontsch, Phys. Rev. D **87**, 114006 (2013) [arXiv:1302.3856 [hep-ph]].
[33] M. Cacciari, G. P. Salam and G. Soyez, Eur. Phys. J. C **72**, 1896 (2012) [arXiv:1111.6097 [hep-ph]].
[34] M. Cacciari, G. P. Salam and G. Soyez, JHEP **0804** (2008) 063 [arXiv:0802.1189 [hep-ph]].
[35] J. de Favereau, C. Delaere, P. Demin, A. Giammanco, V. Lematre, A. Mertens and M. Selvaggi, arXiv:1307.6346 [hep-ex].
[36] J. Alwall, P. Demin, S. de Visscher, R. Frederix, M. Herquet, F. Maltoni, T. Plehn and D. L. Rainwater *et al.*, JHEP **0709** (2007) 028 [arXiv:0706.2334 [hep-ph]]. J. Alwall, M. Herquet, F. Maltoni, O. Mattelaer and T. Stelzer, JHEP **1106** (2011) 128 [arXiv:1106.0522 [hep-ph]].
[37] J. Pumplin, D. R. Stump, J. Huston, H. L. Lai, P. M. Nadolsky and W. K. Tung, JHEP **0207** (2002) 012 [hep-ph/0201195].
[38] M. Bahr, S. Gieseke, M. A. Gigg, D. Grellscheid, K. Hamilton, O. Latunde-Dada, S. Platzer and P. Richardson *et al.*, Eur. Phys. J. C **58** (2008) 639 [arXiv:0803.0883 [hep-ph]].
[39] The ATLAS collaboration, ATLAS-CONF-2013-080 and ATLAS-CONF-2012-135.
[40] The ATLAS collaboration, ATLAS-CONF-2012-043.
[41] T. Junk, Nucl. Instrum. Meth. A **434** (1999) 435. T. Junk, CDF Note 8128 [cdf/doc/statistics/public/8128]. T. Junk, CDF Note 7904 [cdf/doc/statistics/public/7904]. H. Hu and J. Nielsen, in 1st Workshop on Confidence Limits, CERN 2000-005 (2000).
[42] G. Cowan, K. Cranmer, E. Gross and O. Vitells, Eur. Phys. J. C **71**, 1554 (2011).
[43] C. Englert, D. G. Netto, M. Spannowsky and J. Terning, Phys. Rev. D **86** (2012) 035010 [arXiv:1205.0836 [hep-ph]].
[44] A. L. Read, CERN-OPEN-2000-205. A. L. Read, J. Phys. G **G28** (2002) 2693-2704. G. Cowan, K. Cranmer, E. Gross and O. Vitells, Eur. Phys. J. C **71**, 1554 (2011) [arXiv:1007.1727 [physics.data-an]].